

AD-776 673

KINETICS OF Al ATOM OXIDATION

Arthur Fontijn, et al

AeroChem Research Laboratories, Incorporated

Prepared for:

Defense Nuclear Agency
Advanced Research Projects Agency

September 1973

DISTRIBUTED BY:

NTIS

National Technical Information Service
U. S. DEPARTMENT OF COMMERCE
5285 Port Royal Road, Springfield Va. 22151

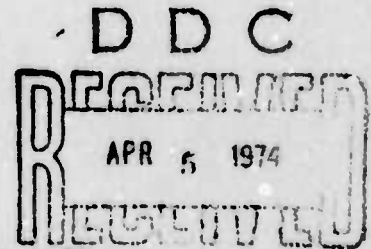
AD776673

KINETICS OF Al ATOM OXIDATION

ARTHUR FONTIJN, WILLIAM FELDER
AND JAMES J. HOUGHTON

AEROCHEM RESEARCH LABORATORIES, INC.
P.O. BOX 12
PRINCETON, NEW JERSEY 08540

September 1973



Final Report for Period 1 May 1972-31 August 1973
CONTRACT NO. DNA 001-72-C-0206-P00001

Approved for public release; distribution unlimited.

THIS WORK SPONSORED BY THE DEFENSE NUCLEAR AGENCY
UNDER SUBTASK 2E50, 3E50

Prepared for

DIRECTOR

DEFENSE NUCLEAR AGENCY

Washington, DC 20305

Reproduced by
NATIONAL TECHNICAL
INFORMATION SERVICE
U S Department of Commerce
Springfield VA 22151

ACCESSION for	
NTIS	Write Section <input checked="" type="checkbox"/>
DDC	Diff Section <input type="checkbox"/>
UNANNOUNCED	<input type="checkbox"/>
JUSTIFICATION	
BY	
DISTRIBUTION AVAILABILITY CODES	
Dist.	Avail. Rec. or Special
A	

"The views and conclusions contained in this document are those of the authors and should not be interpreted as necessarily representing the official policies, either expressed or implied, of the Advanced Research Projects Agency of the U.S. Government."

UNCLASSIFIED

SECURITY CLASSIFICATION OF THIS PAGE (When Data Entered)

REPORT DOCUMENTATION PAGE		READ INSTRUCTIONS BEFORE COMPLETING FORM
1. REPORT NUMBER DNA 3242F	2. GOVT ACCESSION NO.	3. RECIPIENT'S CATALOG NUMBER
4. TITLE (and Subtitle) Kinetics of Al Atom Oxidation		5. TYPE OF REPORT & PERIOD COVERED Final--1 May 1972 to 31 August 1973
		6. PERFORMING ORG. REPORT NUMBER TP-299
7. AUTHOR(s) Arthur Fontijn, William Felder, James J. Houghton		8. CONTRACT OR GRANT NUMBER(s) DNA 001-72-C-0206- P00001 (J104)
9. PERFORMING ORGANIZATION NAME AND ADDRESS AeroChem Research Laboratories, Inc. P.O. Box 12 Princeton, NJ 08540		10. PROGRAM ELEMENT, PROJECT, TASK AREA & WORK UNIT NUMBERS ARPA Order No. 1433 Task Nos. 2E50, 3E50 Work Unit Nos. 12, 02
11. CONTROLLING OFFICE NAME AND ADDRESS Defense Advanced Research Projects Agency 1400 Wilson Boulevard Arlington, VA 22209		12. REPORT DATE September 1973
		13. NUMBER OF PAGES 31
14. MONITORING AGENCY NAME & ADDRESS (if different from Controlling Office) Defense Nuclear Agency Washington, DC 20305		15. SECURITY CLASS. (of this report) Unclassified
		15a. DECLASSIFICATION/DOWNGRADING SCHEDULE
16. DISTRIBUTION STATEMENT (of this Report) Approved for public release; distribution unlimited.		
17. DISTRIBUTION STATEMENT (of the abstract entered in Block 20, if different from Report)		
18. SUPPLEMENTARY NOTES This work was supported by the Defense Nuclear Agency under Subtask M99QAXI002-02.		
19. KEY WORDS (Continue on reverse side if necessary and identify by block number) Al Atoms, Metal Atoms, Chemical Gas Kinetics, Homogeneous Oxidation, Heterogeneous Oxidation, Metal Combustion, Disturbed Atmospheres		
20. ABSTRACT (Continue on reverse side if necessary and identify by block number) The kinetics of the Al/O ₂ reaction system has been studied with the AeroChem high-temperature fast-flow reactor (an adaptation of the steady- state flow reactor suitable for measurements at temperatures up to 2000 K). The rate coefficient for the homogeneous gas-phase reaction $\text{Al} + \text{O}_2 \rightarrow \text{AlO} + \text{O}$ has been determined to be $(3 \pm 2) \times 10^{-11}$ ml molecule ⁻¹ sec ⁻¹ between 1000 and 1700 K. Evidence for a zero-order ($\gamma = (4 \pm 2) \times 10^{-2}$) and a first order wall Al-oxidation process were also obtained. (continued)		

DD FORM 1473

1 JAN 73

EDITION OF 1 NOV 65 IS OBSOLETE

UNCLASSIFIED

SECURITY CLASSIFICATION OF THIS PAGE (When Data Entered)

UNCLASSIFIED

SECURITY CLASSIFICATION OF THIS PAGE(When Data Entered)

Block 20 Abstract (concluded)

A comparison with results obtained on other reactions of the type $\text{Me} + \text{O}_2 \xrightarrow{k_2} \text{MeO} + \text{O}$ (where Me = Fe, U, Sr or Ba) suggests that a value $k_2 = 3 \times 10^{-11} \pm 1 (T/300)^{1/2} \exp(-\Delta H/RT) \text{ ml molecule}^{-1} \text{ sec}^{-1}$ (where ΔH is the endothermicity of the reaction) can be used to estimate k_2 for metal atom species for which no reliable experimental measurements are yet available.

UNCLASSIFIED

SECURITY CLASSIFICATION OF THIS PAGE(When Data Entered)

REPORT SUMMARY

The IVY OWL program requires knowledge of the rate coefficients of metal atom/O₂ reactions and their temperature dependences. A unique type of apparatus, the high-temperature fast-flow reactor (an adaptation of the steady state flow reactor suitable for measurements at temperatures up to 2000 K) developed at AeroChem under earlier contracts, allows the measurement of such rate coefficients. In the preceding ARPA supported work under contract DASA 01-70-C-0152-P00001 (J88), the rate coefficient for the Fe/O₂ reaction was determined at 1600 K. In the present work the rate coefficient of the Al/O₂ reaction has been measured over the 1000 - 1700 K range.

Rate coefficients are obtained from the observed variations in relative metal atom concentration as a function of reaction time, O₂ concentration, total pressure and temperature. In our earlier work, relative metal atom concentration, $[Me]_{rel}$, was obtained via optical absorption measurements of the radiation from (narrow line) hollow cathode lamps. In the course of the present work the apparatus was modified to also allow $[Me]_{rel}$ measurements via fluorescence. Apart from the enhanced confidence in the results provided by a second measurement technique, the ≈ 100 -fold decrease in $[Me]_{initial}$ measurable in fluorescence considerably enhances the versatility of the apparatus by allowing a decrease in temperatures at which reaction rate coefficients can be measured. Thus, the temperature range over which rate coefficients can be obtained, as well as the number of atomic metal species which can be studied, is increased. This reactor modification is discussed in Section II. A, which also contains a discussion of the two types of atomic Al evaporation sources (Al-filled boron nitride crucibles and Al-wetted tungsten wires) developed in the course of this work.

Data were obtained by traversing the O₂ introduction nozzle (located downstream from the metal atom source) and by making fixed nozzle position (time-integrated) measurements. The latter method requires less time to make measurements and was found to give results identical to the former, more accurate, method. The procedures for obtaining rate coefficients in each of these modes from both absorption and fluorescence measurements are discussed in Section II. B.

In Section III the results of the measurements are given and discussed. From measurements over the 10 to 50 Torr pressure, 20 - 120 msec⁻¹ flow velocity range, the homogeneous gas-phase reaction is shown to be



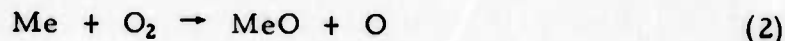
with a rate coefficient of $(3 \pm 2) \times 10^{-11}$ ml molecule⁻¹ sec⁻¹ between 1000 and 1700 K. Evidence was also obtained for heterogeneous oxidation of Al in the

presence of O_2 . Whereas for the Fe/ O_2 system only a heterogeneous process of zero-order in $[O_2]$ was observed, in the Al/ O_2 system: two heterogeneous processes are evident: a process of zero-order in $[O_2]$ with a wall oxidation coefficient, γ , of $(4 \pm 2) \times 10^{-2}$ and another, first order in $[O_2]$, which at the highest $[O_2]$ used proceeds at a rate comparable to the zero-order process. It is speculated that the zero-order process is due to chemisorbed O, while the first-order process is due to adsorbed O_2 in equilibrium with gas-phase O_2 . Although the surfaces encountered in the present work are not identical to those found in environments of ARPA/DNA interest, it is important that calculations on disturbed atmospheres take into account the possibility that, at low pressures, heterogeneous oxidation may dominate. (The transition regime between homogeneous and heterogeneous reaction domination was 1 to 10 Torr in the present work.)

In Section IV the (probably small) T-dependence of k_1 which may have to be considered for extrapolations to lower temperatures, is discussed. We arrive at a recommended value for general calculational use of

$$k_1 = (1.4 \pm 0.9) (T/300)^{1/2} \times 10^{-11} \text{ ml molecule}^{-1} \text{ sec}^{-1}$$

Comparison of this result with the few others available for reactions of the type



suggests that the expression

$$k_2 = 3 \times 10^{-11} \pm 1 (T/300)^{1/2} \exp(-\Delta H/RT) \text{ ml molecule}^{-1} \text{ sec}^{-1},$$

where ΔH is the endothermicity of the reaction, can be used to estimate rate coefficients of metal atom/ O_2 reactions if no reliable experimental measurements are available. For metal atom wall oxidations zero-order in $[O_2]$ $\gamma \approx 10^{-1}$ is the recommended estimate.

FOREWORD

In this final report the results of the experimental work performed under Contract DNA 001-72-C-0206-P00001 (J104) are discussed and general implications for reactions in metal atom/O₂ systems are deduced. The present report incorporates the results previously discussed in an interim report entitled "Kinetics of Metal Atom Oxidation Reactions," DNA 3011Z, AeroChem TN-151, NTIS AD 756 644 (November 1972) by A. Fontijn, W. Felder and J.J. Houghton. The interim report now may be regarded as having been superseded.

TABLE OF CONTENTS

	<u>Page</u>
I. INTRODUCTION	5
II. EXPERIMENTAL	5
A. Apparatus and Materials	5
B. Procedures	9
III. RESULTS AND DISCUSSION	17
IV. CONCLUSIONS AND RECOMMENDATIONS	28
V. REFERENCES	30

LIST OF FIGURESFigure

1	Schematic of the AeroChem High Temperature Fast Flow Reactor	6
2	Cross section of the AeroChem High Temperature Fast Flow Reactor (top view)	7
3	Al-atom concentration profile (absorption)	11
4	Al/O ₂ rate coefficient from k_{ps1} measurements	12
5	Al/O ₂ rate coefficient from fixed nozzle position data (absorption)	13
6	Al-atom concentration profile (fluorescence)	15
7	Plot of measured Al/O ₂ rate coefficients versus pressure at various temperatures	19
8	Plot of measured Al/O ₂ rate coefficients versus pressure at various average gas velocities	20
9	Plot of measured Al/O ₂ rate coefficients versus pressure	21
10	Plot of Al/O ₂ rate coefficient measurements versus pressure	22
11	Plot of all k_{obs} measurements except those obtained at $\bar{v} > 150 \text{ m sec}^{-1}$	24

I. INTRODUCTION

The kinetics of the reaction of O_2 with neutral Al atoms has been measured over the 1000 to 1700 K range. The reactor used is the AeroChem high-temperature fast-flow reactor, suitable for the study of the kinetics of gaseous species at temperatures from about 300 to 2000 K.¹ In earlier work, this reactor was used for the study of the $Fe + O_2 \rightarrow FeO + O$ kinetics at 1600 K.^{2,3} In the course of the present work, the apparatus has been further improved and simplified. It has also been made more versatile by the addition of a third optical port, spaced at 90° from the original two opposing ports, to allow fluorescence measurements to be made. In the apparatus, as used in the present work, Al is vaporized and entrained in an Ar stream; O_2 in excess is introduced through a movable nozzle situated downstream from the Al source (see Fig. 1). Rate coefficients are obtained from the observed variations in relative Al concentration, $[Al]_{rel}$ (measured optically in absorption or fluorescence) as a function of reaction time, $[O_2]$, total pressure and temperature.

II. EXPERIMENTAL

A. Apparatus and Materials

A cross section of the apparatus as presently constituted is shown in Fig. 2. Pt-40% Rh resistance wire is wound directly along the grooved (0.8 cm pitch) outside wall of the 95 cm long, 3.2 cm o.d., 2.5 cm i.d. 998 alumina (99.8% Al_2O_3) reaction tube. A 5.1 cm o.d., 4.5 cm i.d. 998 alumina tube surrounds the reaction tube and serves as the inner support for a Zircar blanket (a flexible zirconium oxide product from Union Carbide)

-
- ¹ Fontijn, A., Kurzius, S.C., Houghton, J.J., and Emerson, J.A., "Tubular Fast Flow Reactor for High Temperature Gas Kinetic Studies," *Rev. Sci. Instr.* 43, 726 (1972).
 - ² Fontijn, A. and Kurzius, S.C., "Tubular Fast-Flow Reactor Studies at High Temperatures. I. Kinetics of the Fe/O_2 Reaction at 1600 K," *Chem. Phys. Lett.* 13, 507 (1972).
 - ³ Fontijn, A., Kurzius, S.C. and Houghton, J.J., "High-Temperature Fast-Flow Reactor Studies of Metal Atom Oxidation Kinetics," Fourteenth Symposium (International) on Combustion (The Combustion Institute, Pittsburgh, 1973), p. 167.

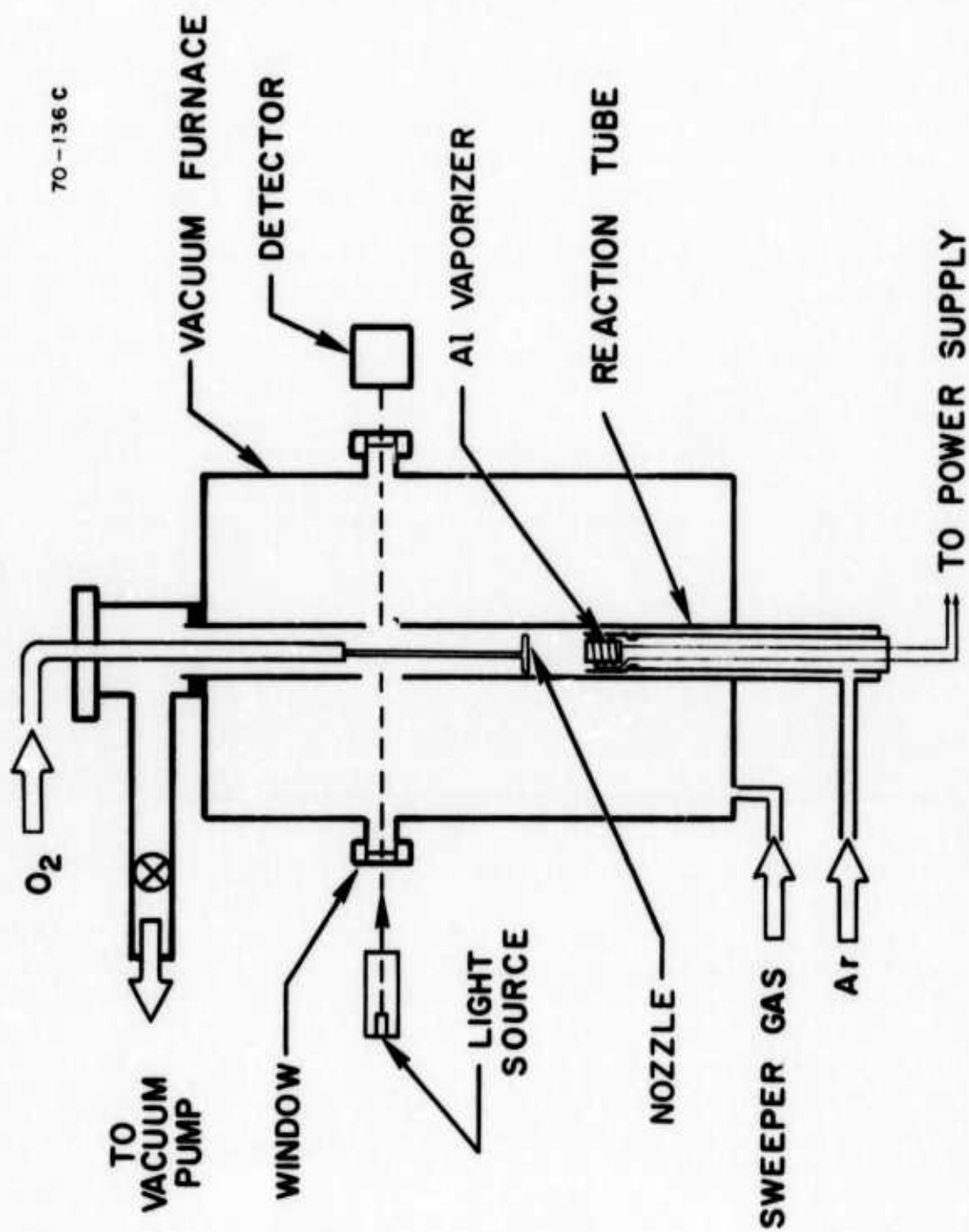


Figure 1. Schematic of the AeroChem High-Temperature Fast-Flow Reactor.

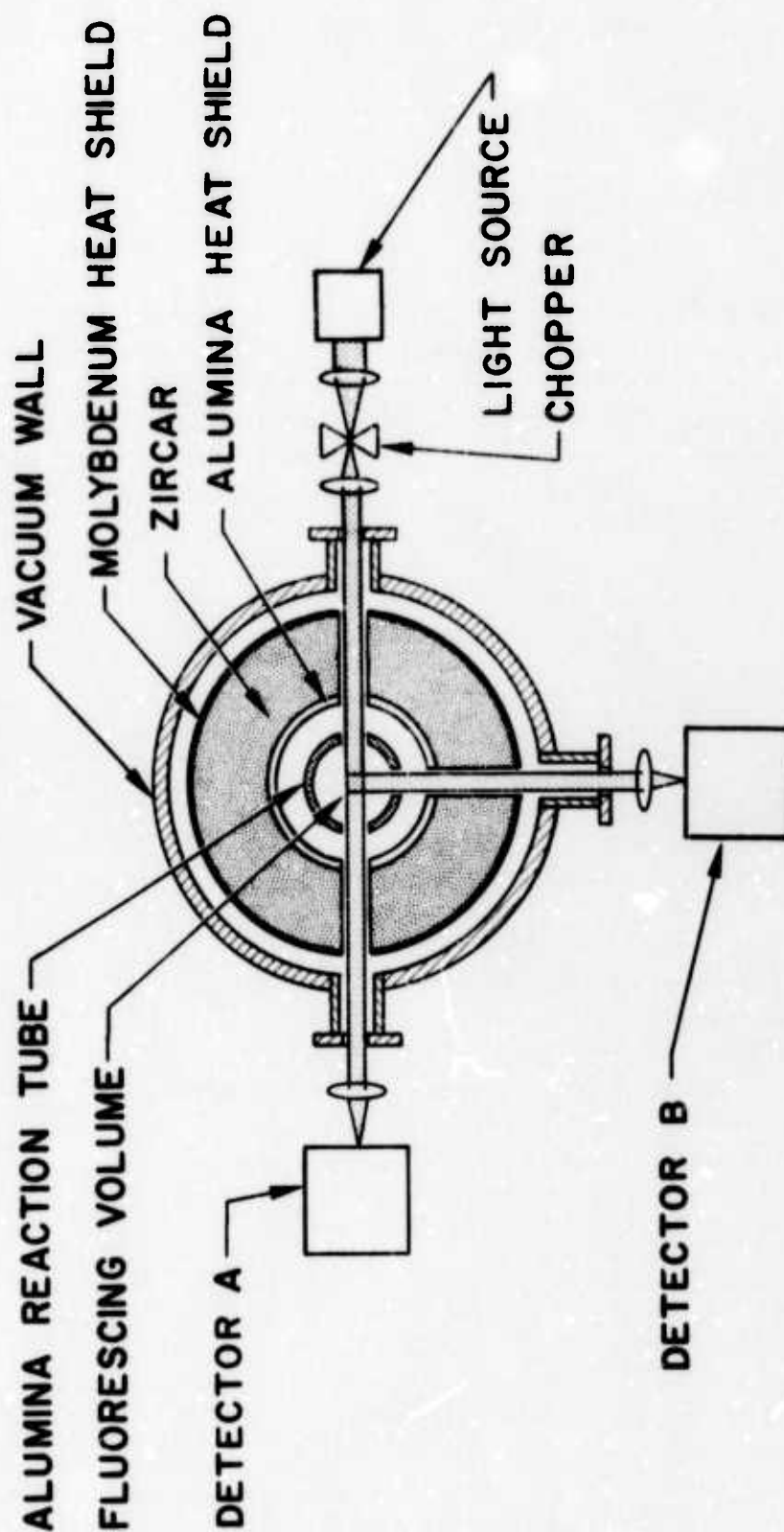


Figure 2. Cross section of the AeroChem High-Temperature Fast-Flow Reactor (top view). Detector A for absorption, Detector B for fluorescence measurements.

which is the principal heat shield. A 15 cm diam cylinder of molybdenum sheet (0.05 cm thick) surrounding the Zircar holds it in place.

This configuration reduces the power consumption of the vacuum furnace considerably from the configuration of Ref. 1, e.g. by a factor of 2 at 1700 K. No resistance wire burn-out or reaction tube fracturing has occurred in the approximately 10 months in which we have continuously used the apparatus in its present form.

The light source indicated in Fig. 1 is a hollow-cathode Al lamp. The detector in the absorption measurements is a 0.5 m Ebert monochromator with an HTV R212 photomultiplier tube. In the fluorescence experiments an EMI 9635QB photomultiplier tube is used in combination with a 303.0 - 314.0 nm bandpass-at-half-width interference filter. The exciting radiation is chopped at 140 Hz and the modulated output of the photomultiplier tubes is detected with a lock-in amplifier.

Two types of Al source were developed and used in the course of this work, resistance heated Al-wetted tungsten wires and Al-filled boron nitride crucibles:

(i) Wires. These were prepared from Mathis Co. F-13 three-stranded helical (7.5×10^{-2} cm diam strands) W coils. Half of every second turn was wrapped with 1.5×10^{-1} cm diam Al (99.999%) wire and the combination was resistance heated in a bell jar under vacuum (0.5 Torr) to above the melting point of Al. Rapid heating to white heat followed by immediate cutoff of the current gave best results. Slow heating results in fragile wires and carries the risk of oxidation. The Al-coated wires were placed on top of the alumina vaporizer tube¹ and fastened to two Mo rods with Pt wire. The Mo rods pass through the vaporizer tube and are connected to a 50 A dc power supply. These wire sources are much easier to prepare than the crucibles and, after introduction into the reactor, yield a stable Al flow through the system in a shorter time than do the crucibles. The wires are the preferred method and were used almost exclusively in the latter part of the work.

(ii) Crucibles. Wide-lipped, 4 cm deep, 1 cm i.d. crucibles, preheated to ≈ 1100 K under vacuum in the bell jar, and brought up to 1 atm pressure with Ar were half-filled with the Al wire. The Ar pressure was then slowly reduced to 1 Torr, and the crucible kept hot until the molten Al stopped bubbling. After cooling, the crucible was placed in the vaporizer tube (with the lip resting on top of this tube) and inserted into the most upstream of the three separately heated contiguous reactor sections. To provide an adequate Al flow, the section containing the Al source was kept at 1600 to 1700 K, independent of the reaction zone temperature used. This procedure was used because direct resistance heating of the crucibles gave less steady Al flows and caused occasional boil-over resulting in resistance wire burn-outs and damage to the reaction tube.

The O₂ inlet (which required frequent replacement) was of the multiperforated distributor ring type described previously.¹ The large rate coefficient of the Al/O₂ reaction makes it necessary to work with small [O₂]. We used 10% O₂ in Ar to obtain conveniently measurable O₂ flow rates. In a few experiments at relatively high [O₂], undiluted O₂ was used with no effect on the results. These gases passed through activated alumina drying columns prior to flowing into the reactor. The bath and sweeper gas Ar were obtained from high purity (99.998% min) liquid Ar containers. 1% O₂ was added to the sweeper gas to (i) remove any Al which could diffuse out of the reaction tube into the sight tubes¹ and (ii) protect the Pt/Rh resistance wire. The sweeper gas volume flow rate was about 10% that of the bath gas. In a few early experiments N₂ rather than Ar bath and sweeper gas was used. The results of rate coefficient measurements obtained using N₂ were consistent with those obtained using Ar; however the raw data were of lower quality and the use of N₂ was discontinued.

B. Procedures

Two methods have been used for obtaining rate coefficients from the measurements of $[Al]_{rel} = [Al]/[Al]_i$. Here, $[Al]_i$ denotes initial Al concentration in the absence of O₂ and $[Al]$ the concentration of Al at the observation port after O₂ addition. In the first (most frequently used) method the O₂ nozzle is traversed along the reactor axis; in the second method it is fixed at a distance x from the observation port. The first method is identical to that discussed in Ref. 3 and yields k_{obs} by way of the intermediate measurement of pseudo-first order rate coefficients, k_{ps1} , via the differential equation $-d[Al]_{rel}/dt = k_{ps1}[Al]_{rel}$, i.e. $k_{ps1} = -d \ln [Al]_{rel}/dt$. From the local slope $a = d \ln [Al]_{rel}/dx$ of the data plots (see Fig. 3), k_{ps1} is obtained via the equation⁴

$$k_{ps1} = \eta a \bar{v} \quad (A)$$

In Eq. (A) η is a factor equal to 1 for plug flow and approximately equal to 1.6 for parabolic flow,⁴ and \bar{v} is the mean bulk linear gas velocity. The right hand side of Eq. A could also include⁵ a factor $(1 + \alpha D_{Al}/\bar{v})$, where D_{Al} is the diffusion coefficient of Al in Ar, to account for back diffusion. However

⁴ Ferguson, E.E., Fehsenfeld, F.C., and Schmeltekopf, A.L., "Flowing Afterglow Measurements of Ion-Neutral Reactions," *Advances in Atomic and Molecular Physics* 5, 1 (1969).

⁵ Kaufman, F., "Reactions of Oxygen Atoms," *Progress in Reaction Kinetics* 1, 1 (1961).

under the conditions of our experiments this factor amounts to at most a few percent correction and was neglected. For our calculations we have taken η to be 1.3 (± 0.3). In general k_{ps_1} contains contributions from a number of terms

$$k_{ps_1} = k_w + k_I[O_2] + k_{II}[O_2][M], \quad (B)^\dagger$$

where k_w is the zero-order wall contribution and k_I and k_{II} are the rate coefficients for binary and ternary Al oxidation. A plot of k_{ps_1} vs. $[O_2]$ has the slope $k_{obs} = k_I + k_{II}[M]$. Such a plot is shown in Fig. 4. When fixed nozzle position data are taken, $[Al]_{rel}$ is plotted directly versus $[O_2]$. The governing time-integrated equation is

$$-\ln[Al]_{rel} = k_w t + k_{obs}[O_2]t \quad (C)$$

Hence the slope of such plots, e.g. Fig. 5, is $k_{obs}t$; k_{obs} is obtained by dividing this quantity by $t = x/\eta \bar{v}$.

In the majority of experiments $[Al]_{rel}$ was measured via absorption (see e.g. Figs. 3 and 5), and in the remainder via fluorescence (see e.g. Fig. 6). In absorption^{2,3} the Lambert-Beer relation is used,

$$[Al]_{rel} \propto \ln(I_0/I), \quad (D)$$

where I_0 and I are the transmitted light intensities in the absence of Al atoms (excess O_2 introduced) and in the presence of Al atoms, respectively. In fluorescence,

$$[Al]_{rel} \propto F/F_i \quad (E)$$

where F and F_i are the fluorescence intensities in the presence and absence of O_2 , respectively. (E) is derived from the expression for fluorescence intensity:

$$F = G I \sigma l [Al] \quad (F)$$

[†] It will be shown in Section III that this general formula should be rewritten to describe our findings on the Al/ O_2 system as

$$k_{ps_1} = k_w + (k_1 + k^*P^{-1})[O_2]$$

where k_1 is the rate coefficient of the homogeneous reaction $Al + O_2 \rightarrow AlO + O$ and k^* a first order wall-recombination coefficient.

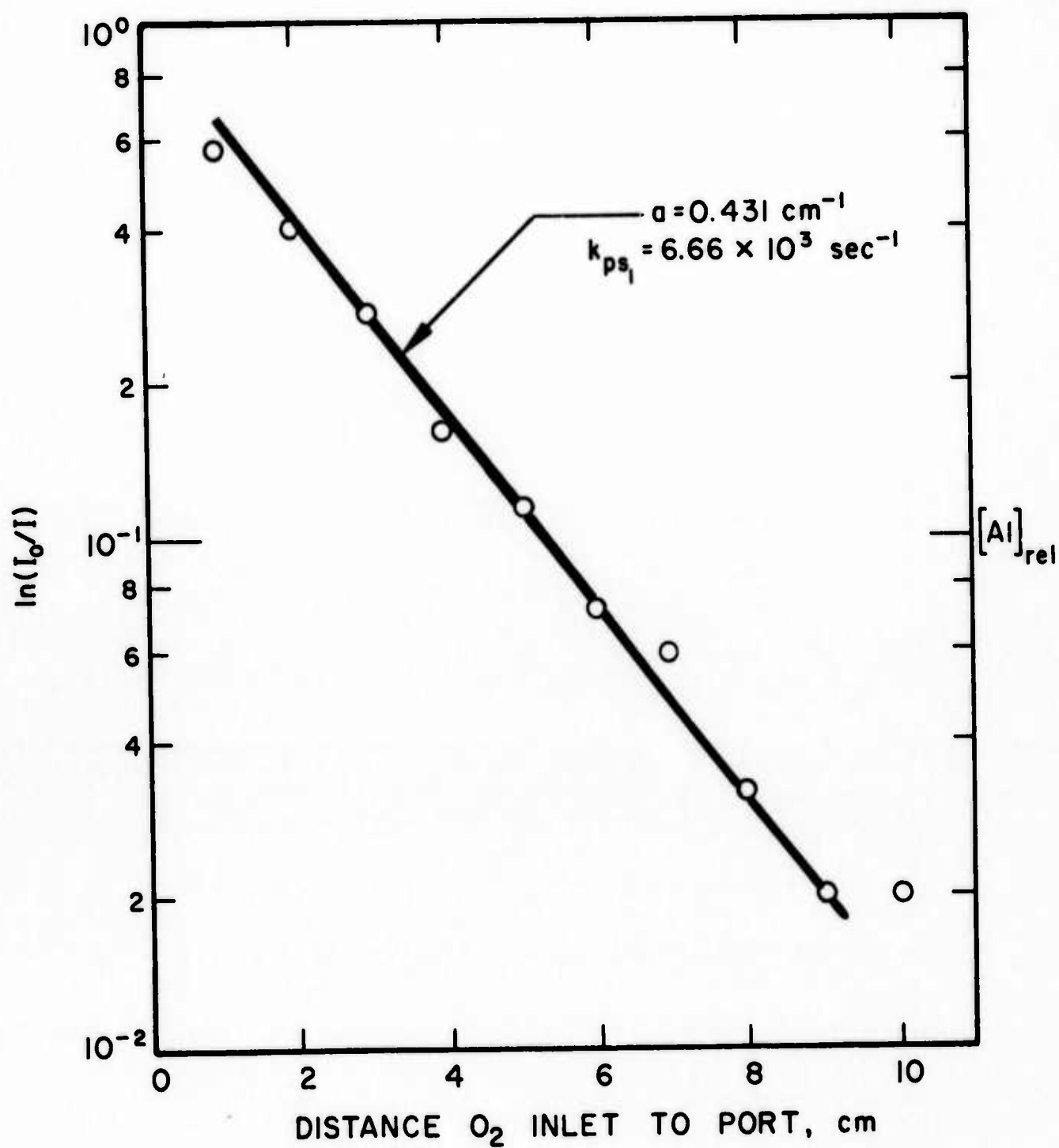


Figure 3. Al-atom concentration profile (absorption). $\bar{T} = 1413 \text{ K}$; $\bar{v} = 118 \text{ msec}^{-1}$; $[O_2] = 12.3 \times 10^{13} \text{ ml}^{-1}$; $\lambda = 394.4 \text{ nm}$; $P = 10 \text{ Torr}$.

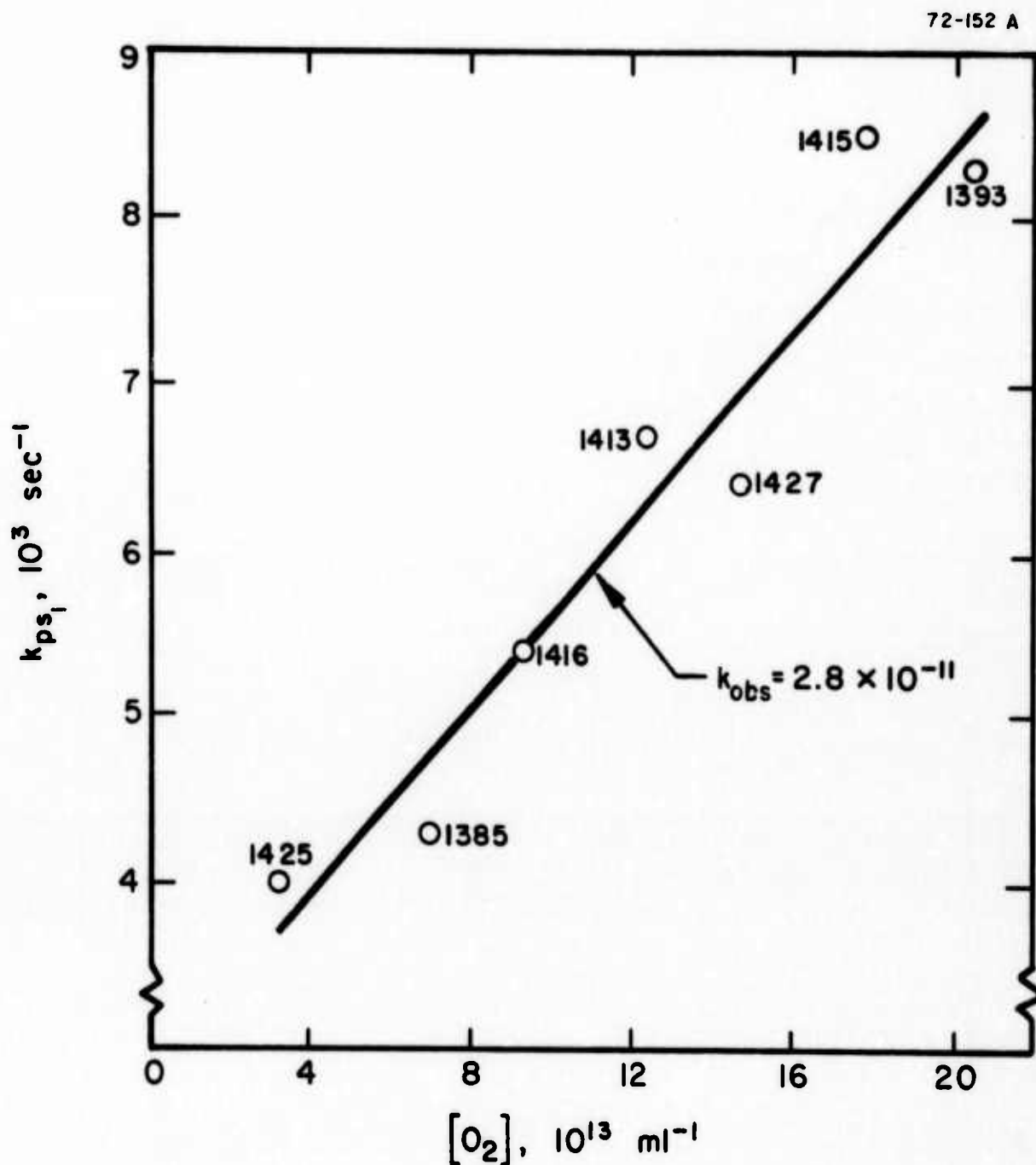


Figure 4. Al/O₂ rate coefficient from k_{ps1} measurements. $\bar{T} = 1411 \text{ K}$; $\bar{v} = 118 \text{ msec}^{-1}$; $\lambda = 394.4 \text{ nm}$; $P = 10 \text{ Torr}$. Numbers beside each individual point indicate the \bar{T} at which it was obtained.

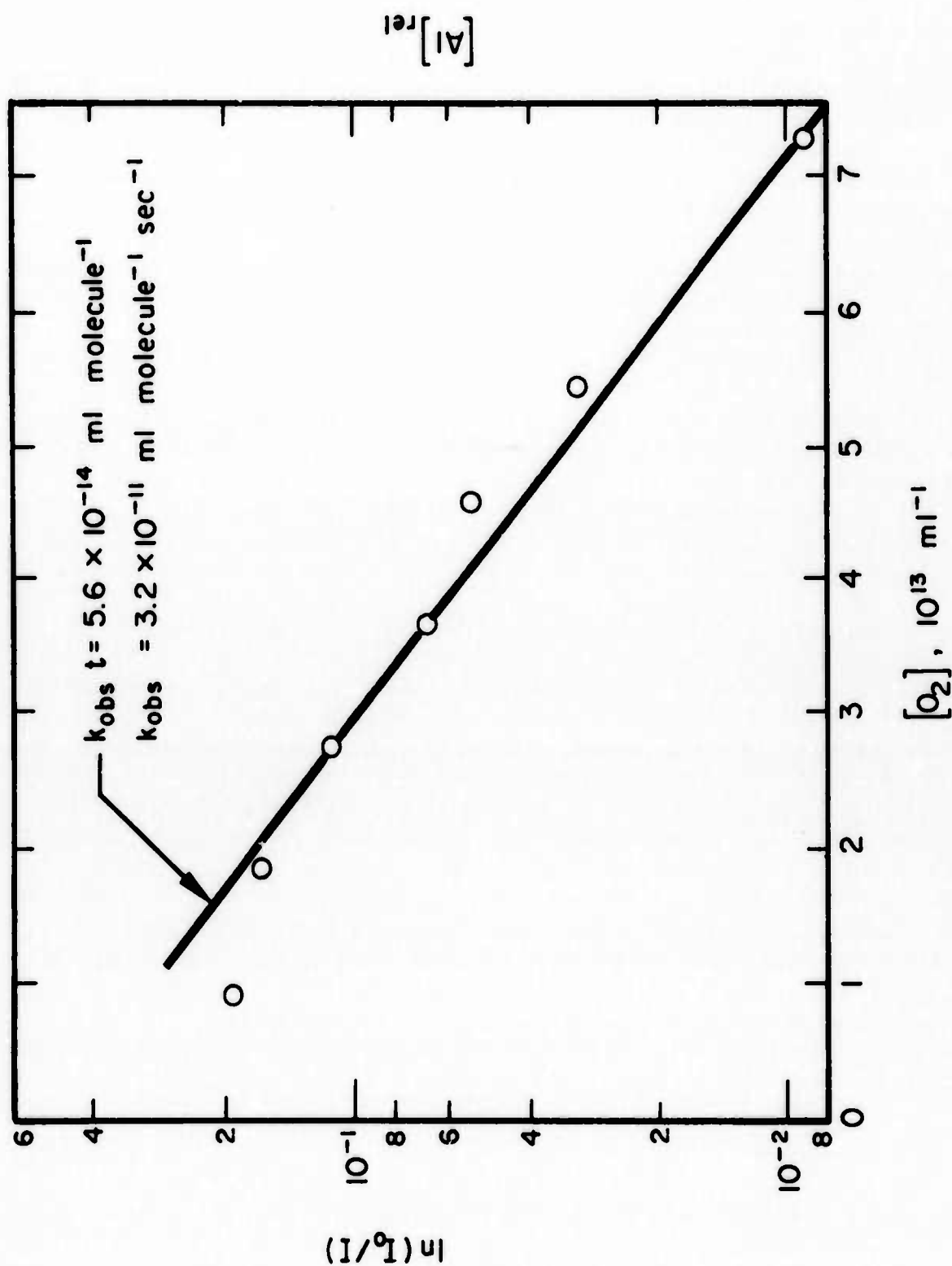


Figure 5. Al/O₂ rate coefficient from fixed nozzle position data (Absorption). $\bar{T} = 1492 \text{ K}$; $\bar{v} = 53 \text{ m sec}^{-1}$; $\lambda = 309.3 \text{ nm}$; $P = 20 \text{ Torr}$; $t = 1.74 \times 10^{-3} \text{ sec}$.

where I is the lamp intensity, σ is the resonance absorption cross section, l is the length of the fluorescing region, and G is a constant instrumental factor which includes the solid angle subtended by the detector, photomultiplier tube (PMT) sensitivity, etc. (F) is valid under optically thin conditions (no re-absorption of the emitted photons) and negligible quenching, but (E) is valid under optically thin conditions provided only that quenching of excited Al atoms before they fluoresce is constant. The constant quenching condition is fulfilled here, as can be seen from the following argument: Under the constant flow conditions of the present measurements, only a change in chemical species can affect the quenching rate, and the only change in species present during a measurement is from Al to AlO and from O_2 to C. Now, $[AlO]$ and $[O]$ are $\approx 10^{12} \text{ ml}^{-1}$ and, even assuming a large quenching rate coefficient of $10^{-10} \text{ ml molecule}^{-1} \text{ sec}^{-1}$, they can affect k_{ps_1} by less than 10^2 sec^{-1} , which is less than 10% of k_{ps_1} (cf. typical values of k_{ps_1} in Figs. 3 and 6). The range of optically thin conditions was determined from a curve-of-growth, i.e. by making a normalized plot of fluorescence intensity versus $[Al]$. At low $[Al]$, the plot is linear with unit slope; at higher densities it deviates due to re-absorption. The linear region is the optically thin range of $[Al]$, which was found to extend to about 35% absorption ($[Al] \approx 10^{11} \text{ ml}^{-1}$, see below).

Two Al lines of different oscillator strength (309.3 nm, $gf = 1.08$ and 394.4 nm, $gf = 0.23$)⁶ were used in the absorption measurements; only the 309.3 nm line was used in the fluorescence studies. Initial Al concentrations giving 50 to 90% absorption were used in the absorption studies. For the fluorescence work $[Al]_i$ values giving 2 to 7% initial absorption were chosen. It follows from the Lambert-Beer equation that the values of $[Al]_i$ used in this work spanned a range of a factor of more than 100. From Linevsky's data,⁷ the highest $[Al]_i$ values used were $\approx 5 \times 10^{12} \text{ ml}^{-1}$ at 394.4 nm and $\approx 1 \times 10^{12} \text{ ml}^{-1}$ at 309.3 nm.

Reaction tube gas stream temperatures were measured with a 0.025 cm diam Pt/Pt-10% Rh thermocouple attached to the movable O_2 inlet. When nozzle traverses were used, T was measured at each nozzle position at which a measurement of $[Al]_{rel}$ was made. \bar{T} is taken as the mean of the gas temperature over the linear region of the data plots, i.e. over the useful length of the reaction tube (compare Figs. 3 and 6), cf. Refs. 1-3. The

⁶ Wiese, W.L., Smith, M.W. and Miles, B.M., Atomic Transition Probabilities, NSRDS-NBS 22, October 1969.

⁷ Linevsky, M.J., "Study of Optical Energy Transfer Processes," General Electric Co., Space Sciences Laboratory, King of Prussia, Pa., RADC-TR-69-97, July 1969.

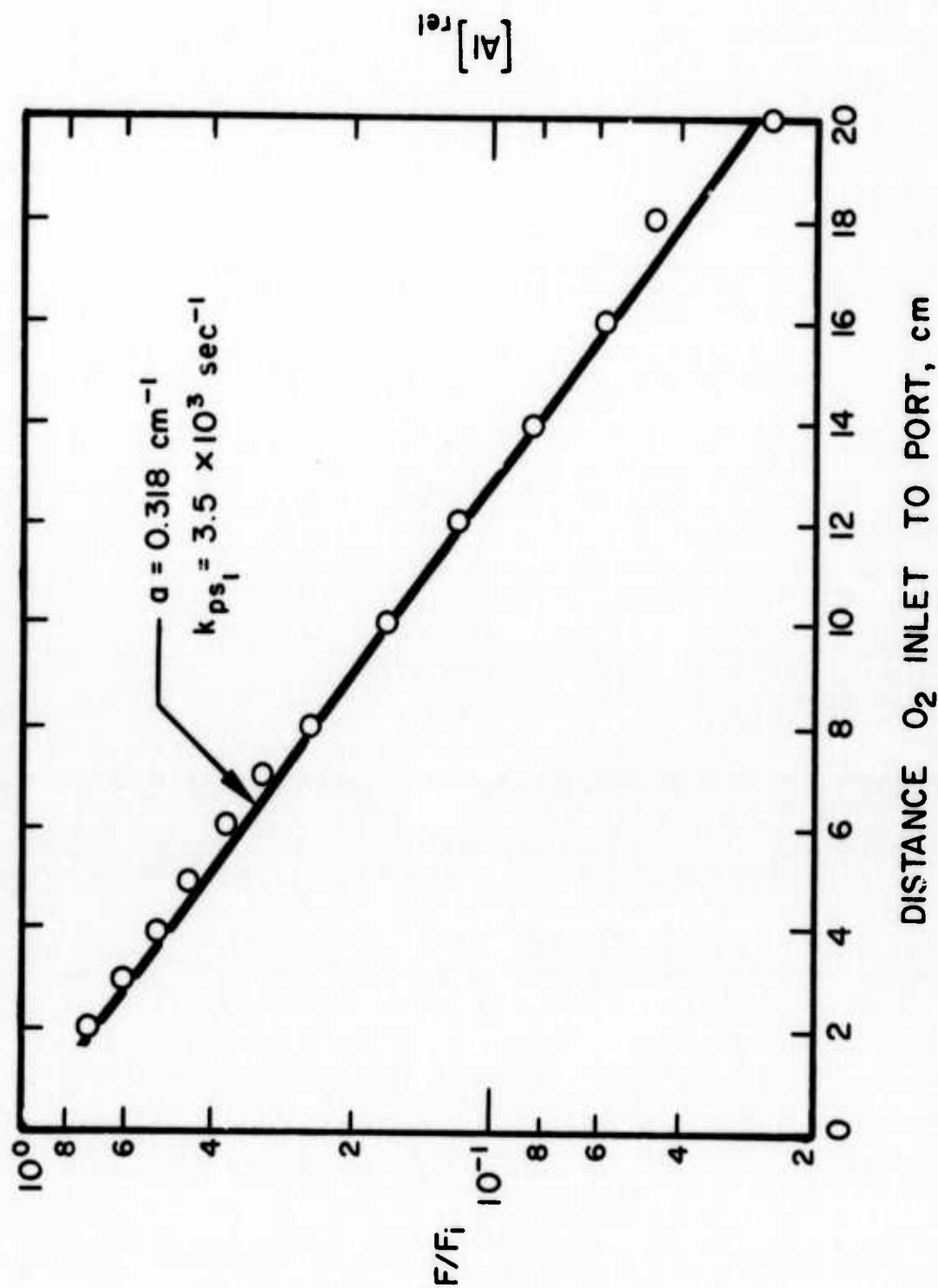


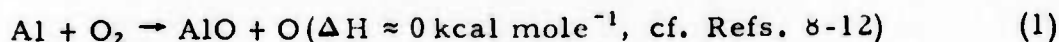
Figure 6. Al-atom concentration profile (fluorescence). $\bar{T} \approx 1085 \text{ K}$; $\bar{v} = 40 \text{ m sec}^{-1}$; $[\text{O}_2] = 6.0 \times 10^{13} \text{ ml}^{-1}$; $\lambda \approx 309.3 \text{ nm}$; $P \approx 10 \text{ Torr}$.

temperature variation over this region was $\pm \approx 25$ K. In experiments using a fixed O_2 inlet position, \bar{T} was determined before O_2 addition by moving the nozzle to positions 12, 7 and 2 cm upstream from the observation ports and then moving it back to the 12 cm position used for the rate coefficient measurement.† In most of this work an effort was made to keep \bar{T} close (± 25 K) to the selected temperatures (1000, 1200, 1400, or 1700 K) by adjusting current flows through each of the three furnace zones. When it became apparent that, within the accuracy of the data, k_{obs} is independent of \bar{T} over this range, this requirement was relaxed, thus considerably reducing the time required to obtain data.

† Measurements were also made at 7 cm from the observation ports, but these were rejected because they showed a marked decrease in the values of their intercepts (cf. Fig. 5) with increasing pressure. The data obtained at 12 cm did not indicate such a trend, indicating that mixing times were sufficiently long to compensate for flow disturbances caused by the observation ports. This is consistent with the "bending over" observed in some plots of $[Al]_{rel}$ versus distance. In such cases, measurements made within a few cm of the observation port indicate an insufficiency of Al (less than the extrapolated straight line value) indicative of mixing inadequacies.

III. RESULTS AND DISCUSSION

The rate coefficients observed and the conditions under which they were obtained are summarized in Table 1. The k_{obs} values measured are plotted against pressure in Figs. 7 to 10. These figures differ in that the shapes of the data points (the cross plots) show the effect of \bar{T} , \bar{v} , the measurement method and the Al-introduction method, respectively; the actual data points are the same in each figure. Figure 7 indicates that k_{obs} is within the accuracy of the data invariant with T over the 1000 - 1700 K range. Figure 8 indicates k_{obs} to be independent of average gas flow velocity at least from 20 to 120 m sec⁻¹; the values at velocities > 150 m sec⁻¹ are not considered further in the analysis because they appear to be consistently somewhat higher than those obtained at the lower velocities (although within the accuracy of the measurements such inclusion would have a negligible effect). Neither Fig. 9 nor 10 shows any dependence of k_{obs} on the cross-plotted quantities. The measurements indicate k_{obs} to be independent of pressure over the 10 to 50 Torr range, indicative of the two-body process:



The mean rate coefficient k_1 obtained from the 10 to 50 Torr data is $3.3 \times 10^{-11} \text{ ml}^3 \text{ molecule}^{-1} \text{ sec}^{-1}$. The normalized standard deviation of this determination of k_1 is 52%. Allowing for a possible 20% systematic error and the 23% uncertainty in $\eta^{2,3}$ the total uncertainty in k_1 is about 60%.

-
- ⁸ JANAF Thermochemical Tables (Dow Chemical Co., Midland, Mich.), June 1971.
 - ⁹ Uy, O.M. and Drowart, J., "Determination by the Mass Spectrometric Knudsen Cell Method of the Atomization Energies of the Gaseous Aluminum Chalcogenides, Al₂, AlCu, AlCuS and AlCuS₂," Trans. Faraday Soc. 67, 1293 (1971).
 - ¹⁰ Farber, M. Srivastava, R.D. and Uy, O.M., "Mass Spectrometric Determination of the Thermodynamic Properties of the Vapor Species From Alumina," J.C.S., Faraday I 68, 249 (1972).
 - ¹¹ Hildenbrand, D.L., "Dissociation Energies of the Molecules AlO and Al₂O," Chem. Phys. Lett. 20, 127 (1973).
 - ¹² Zare, R.N., Columbia University, July 1973 (private communication to A. Fontijn).

TABLE 1. SUMMARY OF THE MEASUREMENTS OF THE RATE COEFFICIENT OF $\text{Al} + \text{O}_2 \rightarrow \text{AlO} + \text{O}$

P (Torr) ^a	$\bar{\nu}$ (cm^{-1})	λ (nm) ^b	$[\text{O}_2]$ (10^{13} ml^{-1})	\bar{T} (K)	k ($10^{-11} \text{ ml mole}^{-1} \text{ sec}^{-1}$)	P (Torr) ^a	$\bar{\nu}$ (cm^{-1})	λ (nm) ^b	$[\text{O}_2]$ (10^{13} ml^{-1})	\bar{T} (K)	k ($10^{-11} \text{ ml mole}^{-1} \text{ sec}^{-1}$)
50	26	A 309.3	0.9 to 5.7	1705	6.7	5.0	218	F 309.3	3.2 to 4.5	1225	11
50	21	A 309.3	3.2 to 9.2	1727	1.9	5.0	190	A 309.3	2.1 to 5.1	1447	11
45	79	A 309.3	1.8 to 12.2	1399	3.0	5.0	190	F 309.3	2.0 to 7.6	1069	8.7
45	40	A 309.3	4.7 to 16	1397	1.1	5.0	188	A 394.4	2.5 to 9.3	1418	6.0
35	53	A 309.3	0.9 to 7.3	1492	3.2	5.0	180	A 309.3	2.1 to 6.2	980	5.2
25	106	A 309.3	1.8 to 7.3	1459	4.5	5.0	176	F 309.3	1.4 to 4.4	1190	10
25	85	A 309.3	3.4 to 11.3	1396	4.2	5.0	92	A 309.3	0.9 to 4.0	1447	10
25	57	A 309.3	6.8 to 17.5	1399	2.2	5.0	92	F 309.3	0.5 to 3.0	1052	9.3
25	42	A 309.3	8.1 to 23	1714	1.0	5.0	90	F 309.3	1.1 to 4.4	1399	8.3
25	40	A 394.4	1.2 to 17.4	1411	2.1	5.0	90	F 309.3	0.5 to 3.2	1409	10
25	40	A 394.4	2.3 to 9.3	1495	1.3	5.0	90	A 309.3	2.1 to 5.3	1429	4.7
20	96	A 309.3	0.3 to 6.7	1500	3.8	5.0	89	A 309.3	2.2 to 9.1	960	4.9
20	26	A 394.4	0.3 to 11.2	1714	2.0	5.0	87	A 309.3	3.3 to 10.6	1406	5.0
15	90	A 309.3	0.5 to 5.5	1460	3.8	5.0	87	A 309.3	3.3 to 11.1	1417	2.4
10	184	A 309.3	2.5 to 10.4	1419	6.6	5.0	51	A 309.3	1.0 to 4.6	1682	9.1
10	119	A 394.4	1.7 to 9.6	1435	6.6	5.0	40	A 309.3	0.6 to 3.6	1421	5.6
10	119	A 394.4	9.3 to 20	1411	2.8	5.0	40	F 309.3	1.1 to 3.0	1026	6.5
10	90	A 309.3	1.1 to 5.3	1431	4.8	5.0	40	A 309.3	2.4 to 12	996	4.1
10	90	F 309.3	2.2 to 5.4	1415	2.7	3.0	90	A 394.4	0.5 to 3.9	1488	17
10	89	A 309.3	1.1 to 4.4	1416	5.4	2.5	53	A 309.3	1.8 to 5.5	1698	11
10	85	A 309.3	2.2 to 11.4	1400	3.2	2.0	380	A 309.3	1.3 to 8.9	1046	8.6
10	80	F 309.3	4.8 to 11.7	1062	2.5	2.0	190	A 309.3	2.0 to 7.6	1064	8.2
10	40	A 309.3	2.4 to 12.3	1392	3.4 ^c	2.0	179	F 309.3	0.7 to 2.2	1201	26
10	20	A 309.3	1.2 to 3.2	1452	4.3	2.0	80	F 309.3	1.8 to 5.2	1012	6.1
6.0	210	A 394.4	2.3 to 9.1	1400	6.0	1.0	216	A 309.3	0.4 to 2.2	1702	130
						1.0	108	A 394.4	0.9 to 4.3	1713	25

^a 1 Torr = 133.3 Nm^{-2} .^b The symbols A and F preceding the wavelengths indicate absorption and fluorescence measurements, respectively.^c N_2 bath gas, Ar used as bath gas in all other series.

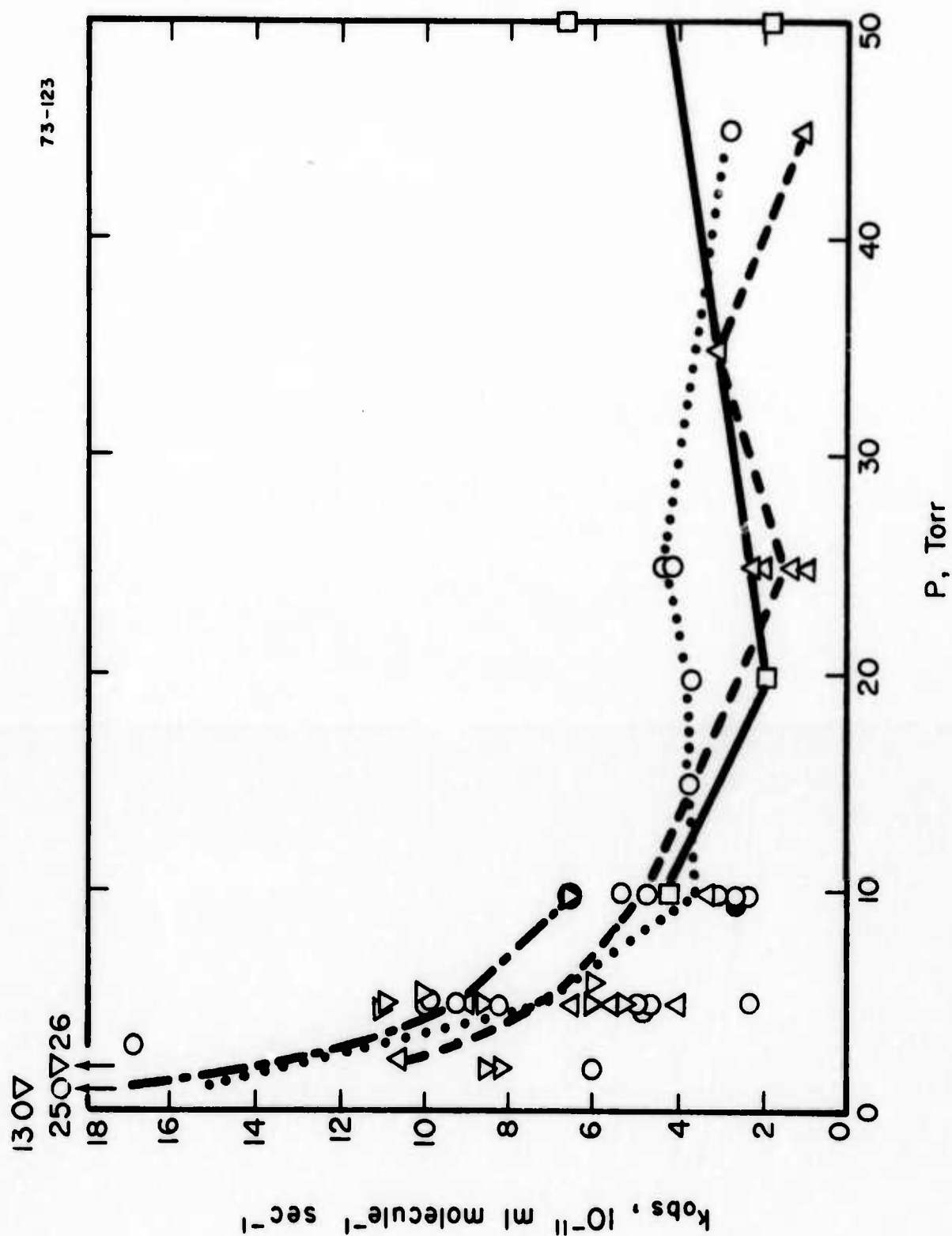


Figure 8. Plot of measured Al/O₂ rate coefficients versus pressure at various average gas velocities. \bar{v} ranges (m sec⁻¹):

\square 20-27 ; Δ 40-57 ; \circ 79-108 ; \bullet 119 ; ∇ > 150

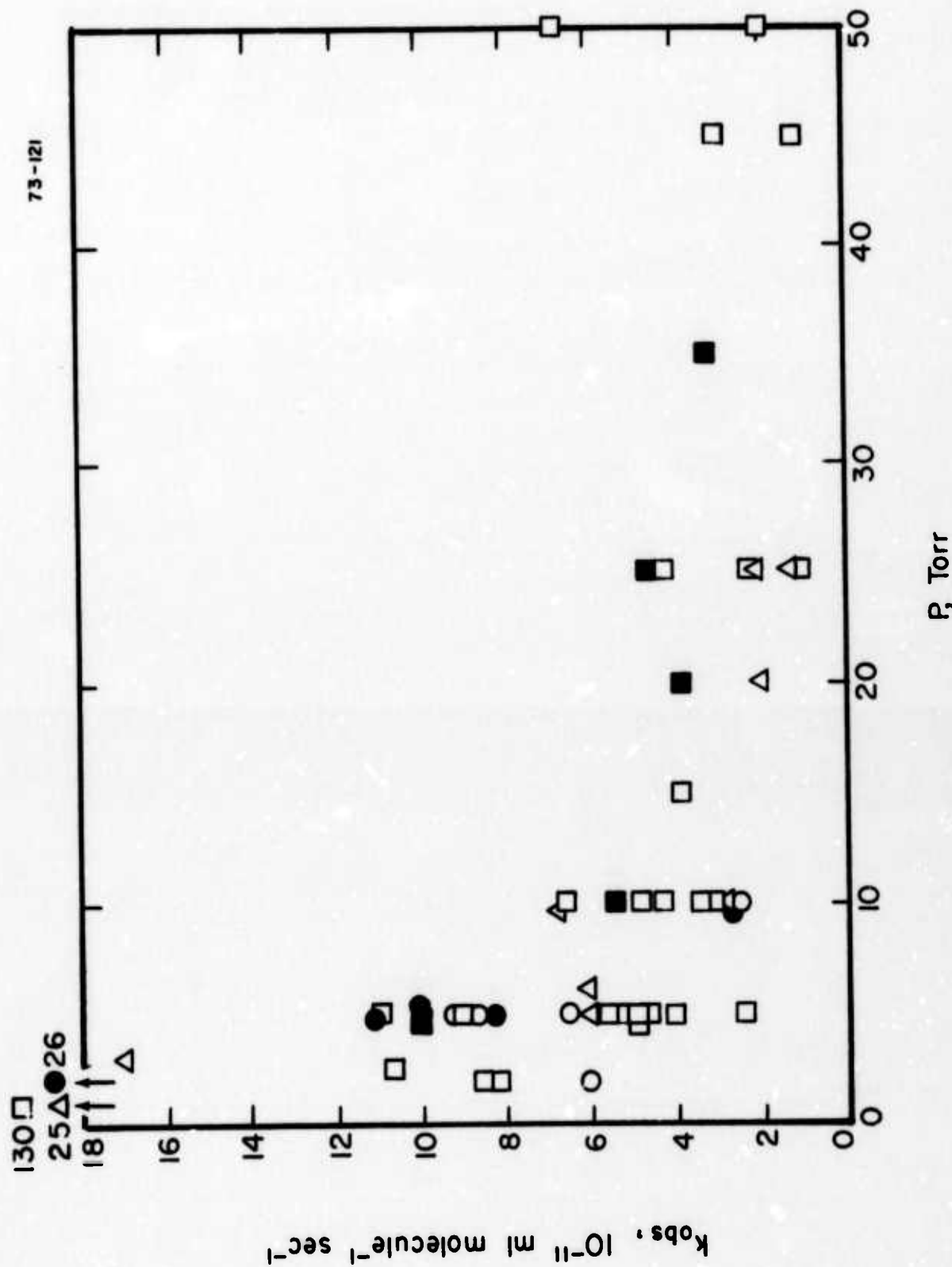


Figure 9. Plot of measured Al/O₂ rate coefficients versus pressure. Data obtained in absorption (\square : 309.3 nm; \triangle 394.4 nm) and fluorescence (\circ : 309.3 nm) and from nozzle traverse (open symbols) and fixed nozzle position (closed symbols) measurements.

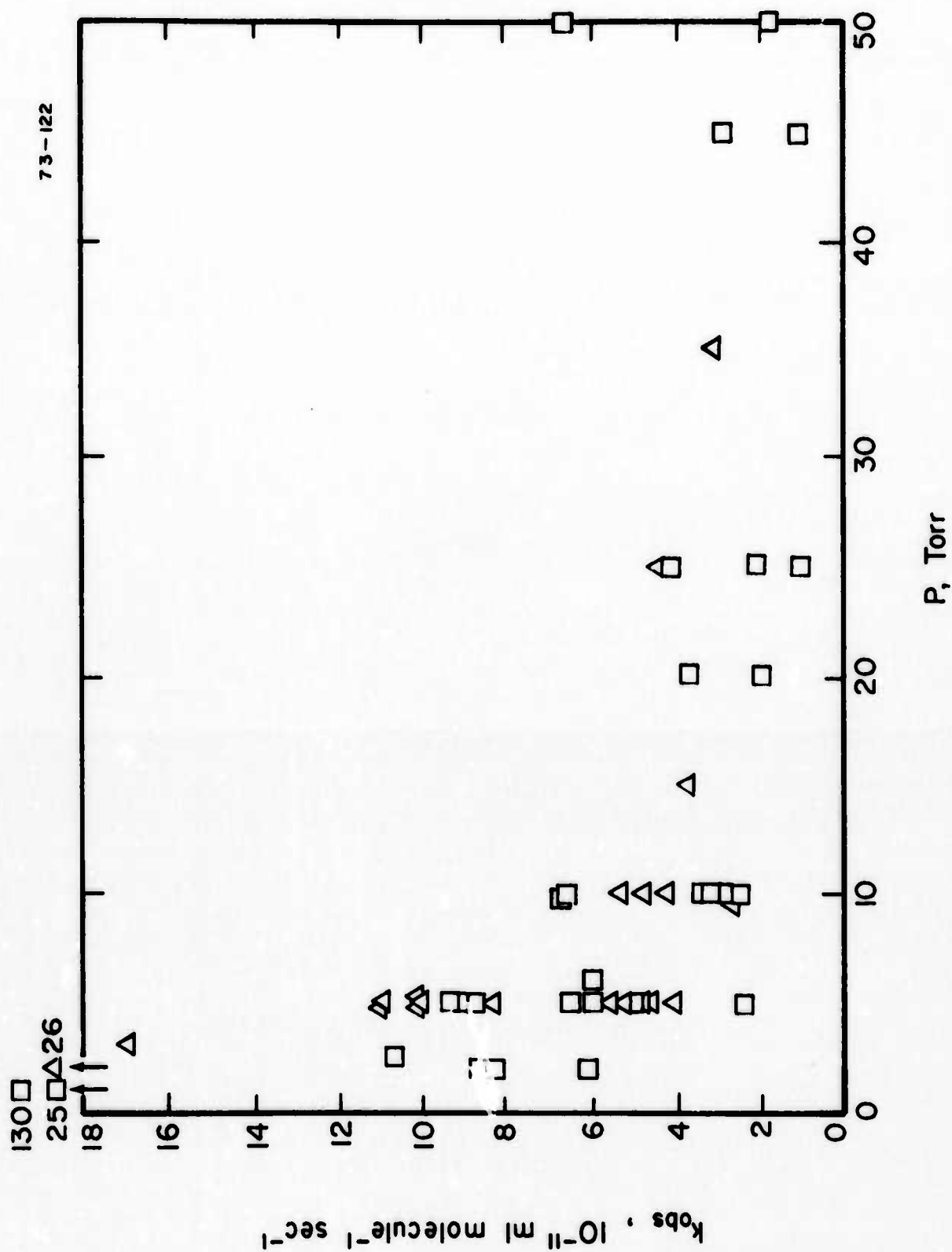


Figure 10. Plot of Al/O₂ rate coefficient measurements versus pressure. Al sources used: \square crucible; Δ W wire.

The increase in k_{obs} at pressures below 10 Torr suggests that the second order term k_I of Eqs. (B) and (C) can be rewritten as

$$k_I = k_1 + k^* P^{-1} \quad (\text{G})$$

A least squares fit of the data to this general formula is shown in Fig. 11. The value of k_1 obtained in this manner is $(3.7 \pm 14\%) \times 10^{-11}$ ml molecule⁻¹ sec⁻¹. The shape of that plot (which still shows perceptible curvature at 10 Torr) suggests yet another method for obtaining k_1 using only data obtained at or above 15 Torr, which would yield $k_1 = (2.9 \pm 55\%) \times 10^{-11}$ ml molecule⁻¹ sec⁻¹. These latter procedures appear somewhat less reliable than the first method since they rely partially on consideration of measurements in a pressure regime where another process (the nature of which is discussed below) is measurably influencing the data. However, within the accuracy of the data it makes essentially no difference which procedure is followed.

Thus, the recommended value for k_1 from the present data is $(3 \pm 2) \times 10^{-11}$ ml molecule⁻¹ sec⁻¹. To our knowledge this measurement constitutes the first experimental determination of k_1 . In view of the approximate thermoneutrality of the reaction, the zero activation energy indicated by the apparent temperature independence of k_1 over the 1000 - 1700 K range is very reasonable.

In the study of the $\text{Fe}/\text{O}_2^{2,3}$ and $\text{Na}/\text{O}_2/\text{M}^3$ reactions, the dominant reaction near 1 Torr was observed to be a rapid wall reaction zero-order in $[\text{O}_2]$, ($\gamma_{\text{Fe}, 1600 \text{ K}} \geq 10^{-1}$; $\gamma_{\text{Na}, 1200 \text{ K}} \approx 10^{-2}$). Zero-order wall reactions were evident also at higher pressures from the positive intercepts of plots of k_{ps_1} vs. $[\text{O}_2]$, i.e. the contribution of k_w of Eq. (B). Although a zero-order reaction is nowhere dominant in the Al/O_2 work at the pressures investigated, its occurrence is again manifested in the intercept of plots such as Figs. 4 and 5. The intercept k_w values measured for the experiments of Table 1 are given in Table 2.[†] Also given in that table are the diffusion-limited^{3,4} values $k_{w,\text{diff}} = 23.2 \text{ d}^{-2} \text{ D}$ and $14.6 \text{ d}^{-2} \text{ D}$ corresponding to plug and parabolic flow, respectively[‡] (d = reaction tube diameter). The diffusion

[†] It should be emphasized that the measurements of heterogeneous oxidation rates were incidental to the present study. The data obtained show considerable scatter, probably due to the fact that prior exposure and age of the reaction tube will have an effect on these rates but cannot be quantitatively accounted for in the analysis.

[‡] Use of these expressions assumes non-turbulent flow which, in the present work is reasonable: Reynolds numbers never exceeded 300.

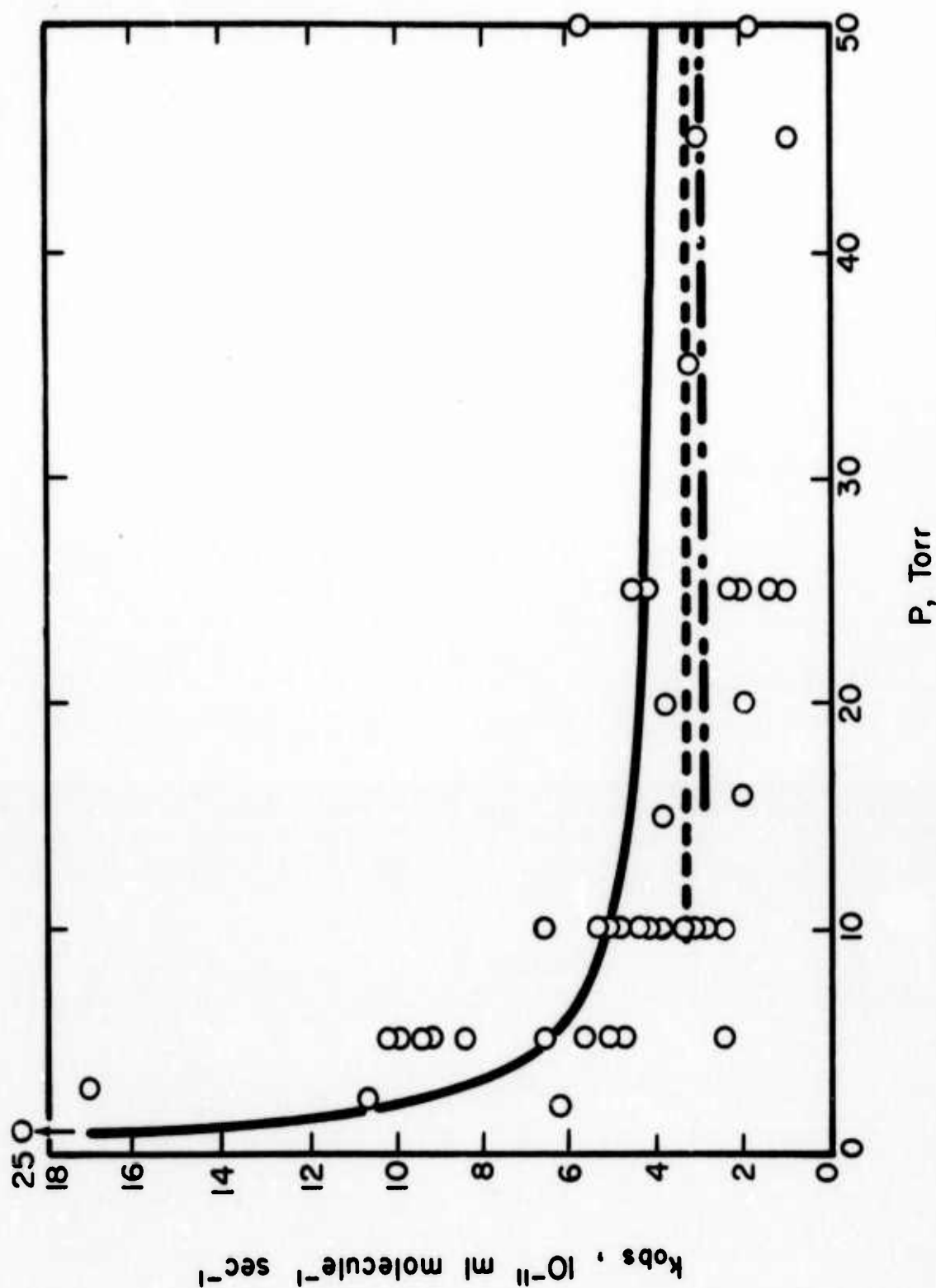


Figure 11. Plot of all k_{obs} measurements except those obtained at $\bar{v} > 150 \text{ m sec}^{-1}$. — Fit to data at all pressures: $k_I = \{ (3.7 \pm 0.5) + (13.7 \pm 9.8) P^{-1} \} \times 10^{-11} \text{ ml molecule}^{-1} \text{ sec}^{-1}$. — — — Mean of $P \geq 10$ Torr data: $k_I = (3.3 \pm 1.7) \times 10^{-11} \text{ ml molecule}^{-1} \text{ sec}^{-1}$. — — — — — Mean of $P \geq 15$ Torr data: $k_I = (2.9 \pm 1.6) \times 10^{-11} \text{ ml molecule}^{-1} \text{ sec}^{-1}$.

TABLE 2. SUMMARY OF MEASUREMENTS OF THE HETEROGENEOUS RATE COEFFICIENTS OF THE Al/O_2 SYSTEM^a

P (Torr)	λ^b (nm)	$[\text{O}_2]_{\text{max}}$ (10^{13} ml^{-1})	\bar{T} (K)	\bar{v} (m sec^{-1})	$k_{w,\text{obs}}$ (10^3 sec^{-1})	$k_{w,\text{diff}} (\text{plug})$ (10^3 sec^{-1})	$k_{w,\text{diff}} (\text{parabolic})$ (10^3 sec^{-1})	$k_w^* P^{-1} [\text{O}_2]_{\text{max}}$ (10^3 sec^{-1})
50	CA 309.3	5.7	1705	26	0.35	0.17	0.11	0.16
50	CA 309.3	9.2	1727	21	0.22	0.17	0.11	0.25
25	CA 309.3	23	1714	42	1.15	0.35	0.22	0.63
20	CA 394.4	11.2	1714	26	1.15	0.43	0.27	0.77
5.0	CA 309.3	4.6	1682	51	1.05	1.7	1.1	1.26
2.5	CA 309.3	5.5	1698	53	1.20	3.5	2.2	3.01
1.0	CA 309.3	2.2	1702	216	2.10	8.7	5.5	3.01
1.0	CA 394.4	4.3	1713	108	2.25	8.7	5.5	5.89
45	CA 309.3	12.2	1399	79	1.40	0.14	0.09	0.37
45	CA 309.3	15.5	1397	40	0.58	0.14	0.09	0.47
35	WA 309.3	7.3	1492	53	1.15	0.19	0.12	0.29
25	WA 309.3	7.3	1489	106	1.11	0.27	0.16	0.40
25	CA 309.3	11.3	1396	85	1.80	0.24	0.15	0.62
25	CA 309.3	17.5	1399	57	0.80	0.24	0.15	0.96
25	CA 394.4	17.4	1411	40	1.48	0.24	0.15	0.95
25	WA 394.4	9.3	1495	40	1.38	0.27	0.16	0.51
20	WA 309.3	6.7	1500	96	2.25	0.31	0.20	0.46
15	WA 309.3	5.5	1460	90	2.55	0.42	0.26	0.50
10	CA 309.3	10.4	1419	184	2.70	0.61	0.38	1.42
10	CA 394.4	9.6	1435	119	3.70	0.61	0.38	1.32
10	CA 394.4	20	1411	119	2.85	0.61	0.38	2.74
10	WA 309.3	5.3	1431	90	1.20	0.61	0.38	0.73
10	WF 309.3	5.4	1415	90	1.35	0.61	0.38	0.71
10	WA 309.3	4.4	1416	89	1.65	0.61	0.38	0.60
10	CA 309.3	11.4	1400	85	2.15	0.61	0.38	1.56
10	WA 309.3	3.2	1452	20	0.53	0.62	0.38	0.44
6.0	CA 394.4	9.1	1400	210	4.25	1.0	0.65	2.08
5.0	WA 309.3	5.1	1447	190	3.20	1.2	0.78	1.40
5.0	CA 394.4	9.3	1418	188	3.25	1.2	0.77	2.55
5.0	WA 309.3	4.0	1417	92	1.01	1.2	0.78	1.10
5.0	WF 309.3	3.2	1409	90	1.80	1.2	0.77	0.88
5.0	WF 309.3	4.4	1399	90	1.40	1.2	0.77	1.21
5.0	WA 309.3	5.3	1429	90	2.80	1.2	0.77	1.45
5.0	CA 309.3	10.6	1406	87	3.25	1.2	0.77	2.90
5.0	CA 309.3	11.1	1117	87	2.25	1.2	0.77	3.04
5.0	WA 309.3	3.6	1421	40	1.20	1.2	0.77	0.99
3.0	WA 394.4	3.9	1488	90	1.50	2.1	1.4	1.78
5.0	WF 309.3	4.5	1225	218	1.65	0.92	0.58	1.23
5.0	WF 309.3	4.4	1190	176	10.	0.92	0.58	1.21
2.0	WF 309.3	2.2	1201	179	2.1	2.3	1.5	1.51
10	CF 309.3	11.7	1062	80	0.78	0.34	0.22	1.60
5.0	CA 309.3	6.2	980	180	4.35	0.66	0.42	1.70
5.0	CF 309.3	5.0	1052	92	0.70	0.67	0.43	0.82
5.0	CA 309.3	9.1	960	89	0.93	0.65	0.41	2.49
5.0	CF 309.3	7.6	1069	87	1.50	0.67	0.43	2.08
5.0	CF 309.3	3.0	1026	40	0.08	0.66	0.42	0.1
5.0	CA 309.3	12	996	40	0.72	0.66	0.42	3.29
2.0	CA 309.3	8.9	1046	380	6.60	1.7	1.0	6.10
2.0	CA 309.3	7.6	1064	190	2.90	1.7	1.0	5.21
2.0	CF 309.3	5.2	1012	179	1.20	1.7	1.0	3.56

^a The individual experiments are the same as those given in Table 1.

^b The first letter preceding the wavelength, C or W, indicates whether a crucible or wire source Al vaporizer was used. The second letter preceding the wavelength, A or F, indicates whether absorption or fluorescence measurements were made.

coefficients of Al in Ar were calculated via the procedures of Reid and Sherwood,¹³ as 2730, 1920, 1450, and 1040 cm² sec⁻¹ at 1 Torr and 1700, 1400, 1200, and 1000 K, respectively. For the four data points obtained at 1700 K and low pressures (1-5 Torr), the observed values, $k_{w,obs}$, are less than the diffusion-limited values allowing the calculation of γ via the usual³ simple kinetic theory formula⁵ $\gamma = k_w / 4 v^{-1}$ (Volume/Surface Area), where v is the mean thermal velocity of the Al atoms. The value of γ thus obtained, taking into account systematic errors and the uncertainty in η , is $(4 \pm 2) \times 10^{-2}$. The values of $k_{w,obs}$ are only, on the average, about a factor 2 less than the diffusion-limited values in the 1-5 Torr range, while $k_{w,obs}$ is larger than $k_{w,diff}$ at higher pressures. It is probable that measurements of γ were possible only near 1700 K because, at those temperatures, the [Al] in the reaction zone did not exceed equilibrium values (the Al vaporizer crucibles were kept at 1600 to 1700 K for experiments at all temperatures, cf. Section II.A). At lower temperatures Al particles, which may act as heterogeneous reaction sites, could form. If Al particles are responsible for the excess surface available then it might be expected that:

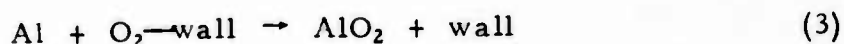
- (i) Data obtained in fluorescence would show a marked decrease in surface effects relative to data obtained in absorption because of the smaller amounts of Al present. For the same reason, but to a lesser degree, a decrease should also be evident in comparing 309.3 to 394.4 nm absorption data.
- (ii) Data obtained using the wire source would show smaller effects due to particles than those obtained using the crucible source since it was found that less Al needed to be evaporated from the source to obtain similar Al concentrations at the observation port; i.e. less Al is available to form particles.

The data show such trends, especially with (ii), although no very marked deviations appear. Reaction sites provided by Al oxide particles might also play a role, since quite possibly the number of such particles also increases with decreasing \bar{T} .

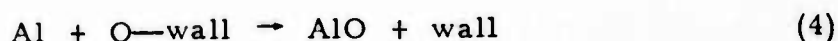
While in the Fe/O₂ work only a zero-order (in [O₂]) wall reaction was evident,³ the increase in k_{obs} (Al/O₂) below 10 Torr (shown in Figs. 7 through 11) is evidence for a heterogeneous reaction first order in [O₂]. From the measured value of k^* (Eq. G and Fig. 11) of this reaction we can calculate a $k_w^* = k^* P^{-1} [O_2]_{max}$ for every row of Table 2. It may be seen from Table 2 that k_w and k_w^* are of similar magnitude.

¹³ Reid, R.C. and Sherwood, T.K., The Properties of Gases and Liquids, 2nd Ed. (McGraw-Hill, 1966), pp. 523-535.

The occurrence of a wall reaction with a rate $\propto [O_2]$ is indicative of surface sites on which the O_2 population is linearly proportional to the gas phase $[O_2]$ (in addition to sites of a different nature where saturation of the oxidant is already achieved at the lowest $[O_2]$ used, i.e. sites of zero-order wall reaction). A possible explanation of this difference can be given by assuming that the first order process is due to reaction of O_2 molecules reversibly adsorbed on the walls



and the zero-order process is due to reaction of chemi-sorbed oxygen



The O formed on the surface would not come rapidly to equilibrium with gas phase O_2 . It is interesting to observe that while free AlO_2 is a known species^{8,10,14} FeO_2 is not known, i.e. FeO is apparently the only possible primary Fe oxidation product (excluding the possibility of a reaction like (3) in the Fe/ O_2 system). The Fe/ O_2 system also differs from the Al/ O_2 system in that FeO formation is strongly endothermic (20 kcal mole⁻¹). It will be interesting to see, when other metal atom/ O_2 reactions are studied in the present type reactor, whether any general correlations of this nature become evident.

¹⁴ Farber, M., Srivastava, R.D. and Uy, O.M., "Mass Spectrometric Determination of the Heat of Formation of the AlO_2 Molecule," J. Chem. Phys. 55, 4142 (1971).

IV. CONCLUSIONS AND RECOMMENDATIONS

In this work the homogeneous gas-phase reaction between Al/O₂ has been shown to proceed via



with a rate coefficient of $(3 \pm 2) \times 10^{-11}$ ml molecule⁻¹ sec⁻¹ with no measurable activation energy. Actually k_1 must have some temperature dependence because of the $T^{1/2}$ factor in the general collision frequency equation. Within the scatter of the experimental data such an effect is too small to be evident from the present 1000 - 1700 K data. Since extrapolation to lower temperatures is of interest to ARPA/DNA, this effect should be taken into account. Taking our k_1 measurement as that for 1350 ± 350 K and expressing it in the general form used in the DNA Reaction Rate Handbook, we obtain

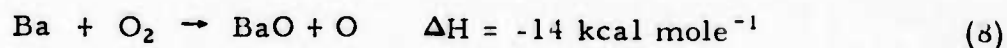
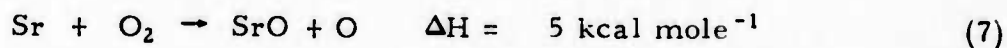
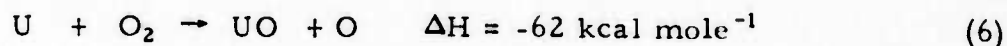
$$k_1 = (1.4 \pm 0.9) (T/300)^{1/2} \times 10^{-11} \text{ ml molecule}^{-1} \text{ sec}^{-1}.$$

There is in principal no reason why our measurements could not be extended to lower temperatures, although the variation looked for would be very small and the accuracy with which data need to be known may not require further measurements. We have performed some exploratory experiments which showed that Al in quantities measurable via fluorescence could be entrained from the source to the observation window at temperatures as low as ≈ 350 K. This temperature is that of the Ar stream heated only by its passage over the crucible Al-source vaporizer; by cooling the reactor temperatures as low as 200 K could probably be investigated.

It is interesting to compare the rate coefficients now available for reactions of the general type



where Me is metal atom. These reactions are, in addition to (1):



k_5 , obtained from our measurement at 1600 K and the assumption that the activation energy equals the endothermicity of the reaction, is^{2,3}
 $2 \times 10^{-10} \exp(-10,000/T)$ ml molecule⁻¹ sec⁻¹. k_6 has been obtained near

room temperature in Fite's thermal beam work¹⁵ as 1×10^{-10} ml molecule⁻¹ sec⁻¹. k_7 and k_8 can be estimated from the velocity-selected crossed-beam work of Batalli-Cosmovici and Michel^{16,17} as $8 \times 10^{-11} \exp(-2650/T)$ and 9×10^{-12} ml molecule⁻¹ sec⁻¹, respectively; k_8 has no measurable T-dependence.¹⁶ Thus the pre-exponential factors of the rate coefficients vary from ≈ 0.03 to 1 times the collision frequency rate coefficient. Generalizing these results, we recommend, for estimates of other reactions of type (2) for which rate coefficients may be required in ARPA/DNA programs, the value $k_2 = 3 \times 10^{-11} \pm 1 (T/300)^{1/2} \exp(-\Delta H/RT)$ ml molecule⁻¹ sec⁻¹, where ΔH is the endothermicity of the reaction. Such estimates are of course considerably less reliable than actual experimental measurements of the rate coefficients. Further confidence in the estimate of k_4 may be obtained from the work of Zare et al^{18,19} which indicates that the rate coefficients for MeO formation in the oxidation of Ca, Sr and Ba by N_2O and NO_2 are of the same magnitude.

Our results indicate that, at 1700 K, zero-order wall oxidation of Al occurs with a γ of $(4 \pm 2) \times 10^{-2}$. Similar γ 's were obtained in our reactor for Fe at 1600 K ($\geq 10^{-1}$) and Na at 1200 K ($\approx 10^{-2}$). Thus zero-order wall recombination with γ 's of 10^{-1} to 10^{-2} appears to be quite common for Me/ O_2 systems. The additional first order heterogeneous oxidation process observed for Al/ O_2 may be exceptional. Its magnitude at $[O_2] = 10^{13}$ to 10^{14} molecule ml⁻¹ is comparable to that of the zero-order heterogeneous process. Though the surfaces in our reaction tube are different from those encountered in systems of ARPA/DNA interest it is useful to realize that under appropriate conditions heterogeneous oxidation rates may exceed homogeneous oxidation rates.

-
- ¹⁵ Fite, W.L., Extranuclear Laboratories, Inc., Pittsburgh, Pa., May 1973 (private communication to A. Fontijn).
 - ¹⁶ Batalli-Cosmovici, C. and Michel, K.W., "Molecular Beam Study on BaO and SrO Formation for Clarifying Interaction of Metal Vapors with Upper Atmosphere Oxygen," Planet. Space Sci. 21, 89 (1973).
 - ¹⁷ Batalli-Cosmovici, C. and Michel, K.W., "Reactive Scattering of a Supersonic O_2 Beam on Ba Atoms," Chem. Phys. Lett. 11, 245 (1971).
 - ¹⁸ Jonah, C.D., Zare, R.N. and Ottinger, Ch., "Crossed-Beam Chemiluminescence Studies of Some Group IIa Metal Oxides," J. Chem. Phys. 56, 263 (1972).
 - ¹⁹ Ottinger, Ch. and Zare, R.N., "Crossed Beam Chemiluminescence," Chem. Phys. Lett. 5, 243 (1970).

REFERENCES

1. Fontijn, A., Kurzius, S.C., Houghton, J.J., and Emerson, J.A., "Tubular Fast-Flow Reactor for High Temperature Gas Kinetic Studies," *Rev. Sci. Instr.* 43, 726 (1972).
2. Fontijn, A. and Kurzius, S.C., "Tubular Fast-Flow Reactor Studies at High Temperatures. I. Kinetics of the Fe/O₂ Reaction at 1600 K," *Chem. Phys. Lett.* 13, 507 (1972).
3. Fontijn, A., Kurzius, S.C. and Houghton, J.J., "High-Temperature Fast-Flow Reactor Studies of Metal Atom Oxidation Kinetics," Fourteenth Symposium (International) on Combustion (The Combustion Institute, Pittsburgh, 1973), p. 167.
4. Ferguson, E.E., Fehsenfeld, F.C. and Schmeltekopf, A.L., "Flowing Afterglow Measurements of Ion-Neutral Reactions," *Advances in Atomic and Molecular Physics* 5, 1 (1969).
5. Kaufman, F., "Reactions of Oxygen Atoms," *Progress in Reaction Kinetics* 1, 1 (1961).
6. Wiese, W.L., Smith, M.W. and Miles, B.M., Atomic Transition Probabilities, NSRDS-NBS 22, October 1969.
7. Linevsky, M.J., "Study of Optical Energy Transfer Processes," General Electric Co., Space Sciences Laboratory, King of Prussia, Pa., RADC-TR-69-97, July 1969.
8. JANAF Thermochemical Tables (Dow Chemical Co., Midland, Mich.), June 1971.
9. Uy, O.M. and Drowart, J., "Determination by the Mass Spectrometric Knudsen Cell Method of the Atomization Energies of the Gaseous Aluminum Chalcogenides, Al₂, AlCu, AlCuS and AlCuS₂," *Trans. Faraday Soc.* 67, 1293 (1971).
10. Farber, M., Srivastava, R.D. and Uy, O.M., "Mass Spectrometric Determination of the Thermodynamic Properties of the Vapor Species from Alumina," *J.C.S., Faraday I* 68, 249 (1972).
11. Hildenbrand, D.L., "Dissociation Energies of the Molecules AlO and Al₂O," *Chem. Phys. Lett.* 20, 127 (1973).

12. Zare, R.N., Columbia University, July 1973 (private communication to A. Fontijn).
13. Reid, R.C. and Sherwood, T.K., The Properties of Gases and Liquids, 2nd Ed. (McGraw-Hill, 1966), pp. 523-535.
14. Farber, M., Srivastava, R.D. and Uy, O.M., "Mass Spectrometric Determination of the Heat of Formation of the AlO_2 Molecule," J. Chem. Phys. 55, 4142 (1971).
15. Fite, W.L., Extranuclear Laboratories, Inc., Pittsburgh, Pa., May 1973 (private communication to A. Fontijn).
16. Batalli-Cosmovici, C. and Michel, K.W., "Molecular Beam Study on BaO and SrO Formation for Clarifying Interaction of Metal Vapors with Upper Atmosphere Oxygen," Planet. Space Sci. 21, 89 (1973).
17. Batalli-Cosmovici, C. and Michel, K.W., "Reactive Scattering of a Supersonic O_2 Beam on Ba Atoms," Chem. Phys. Lett. 11, 245 (1971).
18. Jonah, C.D., Zare, R.N. and Ottinger, Ch., "Crossed-Beam Chemiluminescence Studies of Some Group IIa Metal Oxides," J. Chem. Phys. 56, 263 (1972).
19. Ottinger, Ch. and Zare, R.N., "Crossed Beam Chemiluminescence," Chem. Phys. Lett. 5, 243 (1970).